Ecological Applications, 18(8) Supplement, 2008, pp. A239–A256

CLEAR LAKE SEDIMENTS: ANTHROPOGENIC CHANGES IN PHYSICAL SEDIMENTOLOGY AND MAGNETIC RESPONSE

David A. Osleger,[1,5] Robert A. Zierenberg,[1] Thomas H. Suchanek,[2,6] Joseph S. Stoner,[3] Sally Morgan,[4] and David P. Adam[2,7]

[1]*Department of Geology, University of California, Davis, California 95616 USA*
[2]*Department of Wildlife, Fish and Conservation Biology, University of California, Davis, California 95616 USA*
[3]*College of Oceanic and Atmospheric Sciences, Oregon State University, Corvallis, Oregon 97331 USA*
[4]*School of Earth and Environment, University of Leeds, Leeds LS2 9JT United Kingdom*

Abstract. We analyzed the sedimentological characteristics and magnetic properties of cores from the three basins of Clear Lake, California, USA, to assess the depositional response to a series of land use changes that occurred in the watershed over the 20th century. Results indicate that distinct and abrupt shifts in particle size, magnetic concentration/mineralogy, and redox conditions occur concurrently with a variety of ecological and chemical changes in lake bed sediments. This coincidence of events occurred around 1927, a datum determined by an abrupt increase in total mercury (Hg) in Clear Lake cores and the known initiation of open-pit Hg mining at the Sulphur Bank Mercury Mine, confirmed by ^{210}Pb dating. Ages below the 1927 horizon were determined by accelerator mass spectrometry on ^{14}C of coarse organic debris. Calculated sedimentation rates below the 1927 datum are ~1 mm/yr, whereas rates from 1927 to 2000 are up to an order of magnitude higher, with averages of ~3.5–19 mm/yr.

In both the Oaks and Upper Arms, the post-1927 co-occurrence of abrupt shifts in magnetic signatures with color differences indicative of changing redox conditions is interpreted to reflect a more oxygenated diagenetic regime and rapid burial of sediment below the depth of sulfate diffusion. Post-1927 in the Oaks Arm, grain size exhibits a gradual coarsening-upward pattern that we attribute to the input of mechanically deposited waste rock related to open-pit mining activities at the mine. In contrast, grain size in the Upper Arm exhibits a gradational fining-upward after 1927 that we interpret as human-induced erosion of fine-grained soils and chemically weathered rocks of the Franciscan Assemblage by heavy earthmoving equipment associated with a road- and home-building boom, exacerbated by stream channel mining and wetlands destruction. The flux of fine-grained sediment into the Upper Arm increased the nutrient load to the lake, and that in turn catalyzed profuse cyanobacterial blooms through the 20th century. The resulting organic biomass, in combination with the increased inorganic sediment supply, contributed to the abrupt increase in sedimentation rate after 1927.

Key words: Clear Lake, California, USA; ^{14}C; land use patterns; late Holocene; magnetite dissolution; mercury; paleolimnology; particle size trends; Sulphur Bank Mercury Mine.

Introduction

Recent studies of sediment cores from Clear Lake, California, USA, document several coincident and abrupt changes in chemical parameters in the upper few meters of lake bed sediments (e.g., Richerson et al. 1994, 2000, 2008, Suchanek et al. 2008*b*). Total mercury (TotHg), methylmercury (MeHg), organic matter, water content, total carbon, total nitrogen, total phosphorus, and total sulfur all exhibit significant shifts from background levels beginning at ~30–140 cm depth in the cores (Richerson et al. 2008). The sharp increase in these parameters in all cores is estimated to have occurred around 1927, confirmed to an acceptable degree of accuracy by ^{210}Pb dating (Richerson et al. 2008). This date marks the beginning of open-pit Hg mining from the Sulphur Bank Mercury Mine located on the east end of the Oaks Arm of the lake (Fig. 1). Furthermore, sedimentation rates calculated for post-1927 sediments are up to an order of magnitude higher than rates calculated for sediment accumulation pre-1927. This major increase in sedimentation rates throughout the lake, as well as the concurrent environmental changes reflected in the other chemical indicators, are very likely related to the advent of open-pit mining as well as the use of heavy earthmoving equipment associated with local watershed development beginning in the late 1920s (Richerson et al. 2000, 2008).

If these anthropogenic changes in the Clear Lake watershed did influence erosion/sedimentation rates,

Manuscript received 4 September 2006; revised 26 June 2007; accepted 30 July 2007; final version received 2 October 2007. Corresponding Editor (ad hoc): B. Henry. For reprints of this Special Issue, see footnote 1, p. A1.

[5] E-mail: osleger@geology.ucdavis.edu

[6] Present address: Western Ecological Research Center, U.S. Geological Survey, 3020 State University Drive East, Sacramento, California 95819 USA.

[7] Present address: 18522 Sentinel Court, Hidden Valley Lake, California 95467 USA.

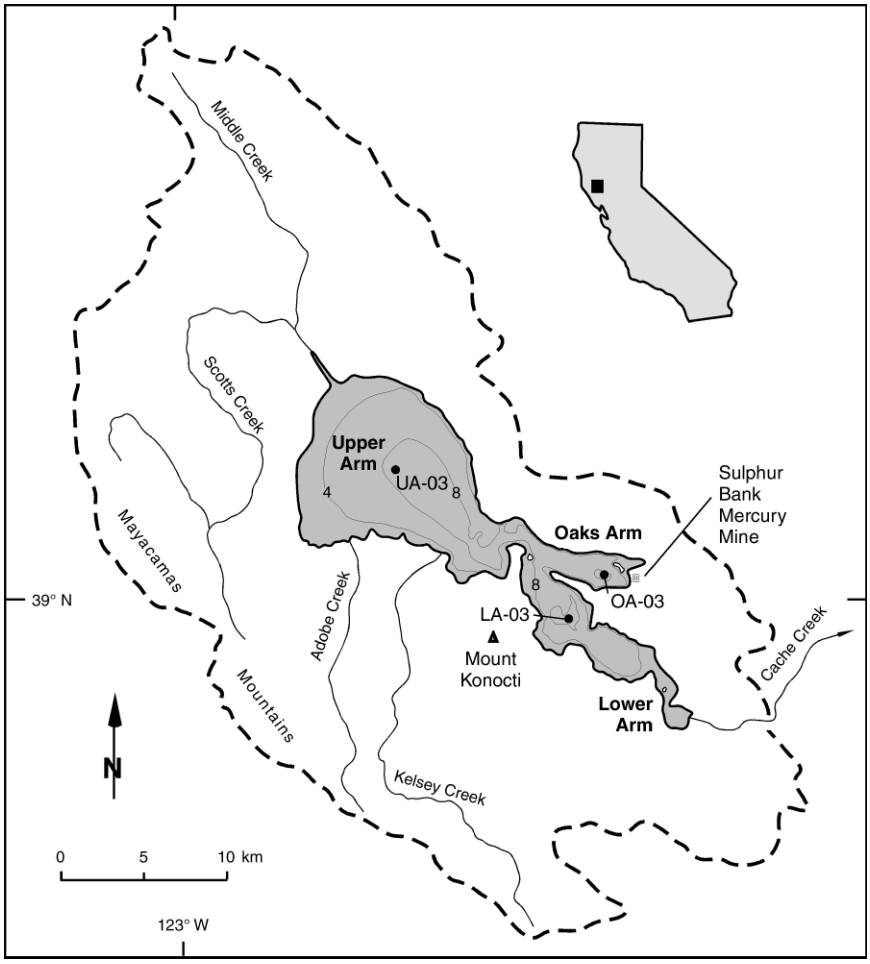

FIG. 1. Location of Clear Lake, California, showing watershed boundaries, major streams, lake bathymetry (after Goldman and Wetzel 1963; depth in meters), and location of cores used in this study.

there should be corresponding changes recorded in the textural and magnetic properties of the lake bed sediments. In this study, we measured the sedimentologic and magnetic characteristics of sediment cores to evaluate the depositional response to a variety of land use activities in the Clear Lake basin through the 20th century. Lead-210 (^{210}Pb) dating, tied to Hg profiles (Richerson et al. 2008: Table 1), provides the age control in the uppermost section of the cores used in this study. Peaks in the dichlorodiphenyldichloroethane (DDD) concentration of near-surface sediments constrain more recent changes in sediment accumulation rates (Richerson et al. 2008). Sediments in the lower portions of the cores used in this study were dated by accelerator mass spectrometry (AMS) on ^{14}C of woody organic debris deposited with the sediments. Results of our study indicate that depositional processes changed rapidly, concurrent with the abrupt shifts in chemical and ecological parameters beginning around 1927, adding support for hypothesized environmental changes wrought by the advent of open-pit mining and widespread watershed development.

This paper documents the fundamental depositional and diagenetic framework upon which the other papers in this volume are based and provides first-order evidence for the increased flux of sediment and associated nutrients to the lake since large-scale anthropogenic changes began in the watershed around 1927. Furthermore, radiocarbon dates and sedimentation rates laid out in this paper provide the age control for several other papers in this volume.

Environmental Setting and Methods

Clear Lake is a shallow, eutrophic lake located in the Coast Range of northern California in a region of active tectonism and recent volcanism (Sims et al. 1988; Fig. 1). Roughly 60% of the land area in the Clear Lake drainage basin is underlain by greywackes, shales, and cherts of the Franciscan Assemblage, whereas ~13% is underlain by Clear Lake volcanics that range in age from 2.1×10^6 yr (Ma) to 10×10^3 yr (ka; Sims et al.

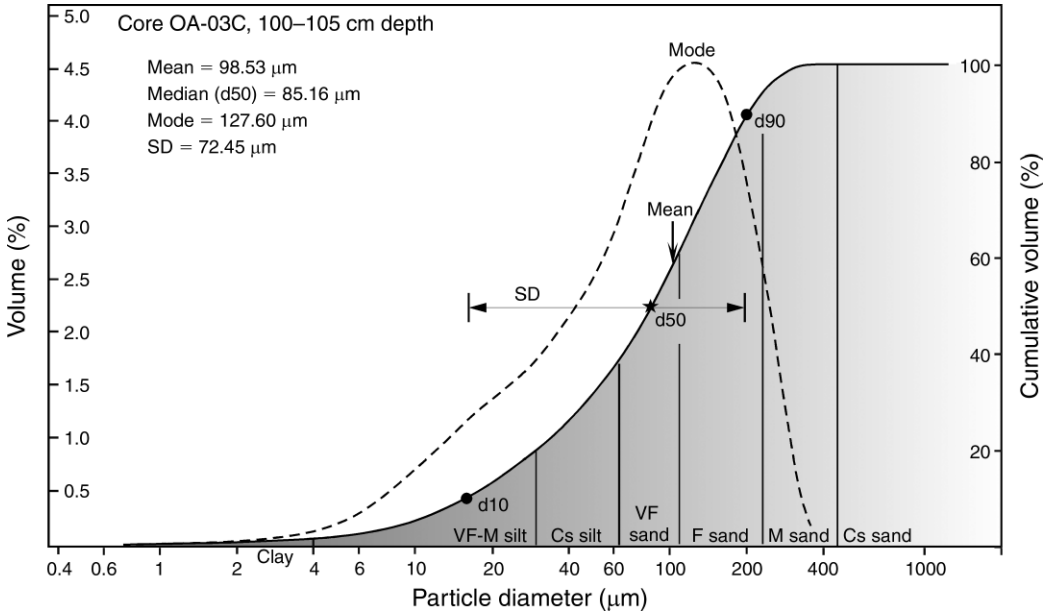

FIG. 2. Graphic presentation of particle size parameters that were measured on the laser diffractometer. The example shown is from sediment homogenized from the 100–105 cm interval in core OA-03C. The dashed curve represents the individual volume percentage for each specific size fraction. The solid curve is the cumulative volume percentage distribution from which d10, d50, and d90 are measured. The d50 value represents the median grain diameter, whereas d10 and d90 represent the grain diameters at the 10th and 90th percentile values. As defined on the Udden-Wentworth grain size scale, abbreviations are: VF, very fine; F, fine; M, medium; and Cs, coarse.

1988). The remainder of the drainage basin consists of streams and floodplains covered with a veneer of Quaternary alluvium derived from the adjacent rocks. Approximately 90% of the seasonal influx of water flows into the Upper Arm through streams that drain primarily the Franciscan and Quaternary deposits of the watershed (Richerson et al. 1994). Relatively small seasonal inflows occur into the Oaks and Lower Arms of the lake. The present outflow is entirely through Cache Creek at the southern end of the Lower Arm.

Cores up to ~2.5 m sediment depth were recovered from all three arms of the lake using a push-rod piston corer in September 2000 (Fig. 1) collected from a 6.7-m research vessel. Two cores were collected immediately adjacent to one another in the Lower (LA-03A, LA-03B) and Upper Arms (UA-03A, UA-03B). Three cores were collected from the Oaks Arm (OA-03A, OA-03B, OA-03C). Core OA-03B is significantly shorter than the adjacent cores, likely due to over-penetration during coring operations.

Sediment from cores UA-03A, OA-03A, OA-03C, and LA-03A was sampled at 5-cm increments (2.5-cm intervals for the uppermost 50 cm) and homogenized for a variety of analyses, including most of the chemical parameters discussed elsewhere in this volume (Richerson et al. 2008, Suchanek et al. 2008*a*). Subsamples of these 5-cm increments from cores UA-03A, OA-03C, and LA-03A were used in this study for grain size analysis and scanning electron microscopy (SEM). For the grain size analysis, samples from each interval were placed in a vial and disaggregated using a sodium metaphosphate solution. The samples were shaken overnight to insure dispersion, and each sample was run on a Coulter LS-230 laser diffractometer (Coulter, Fullerton, California, USA). The resulting digital file records a variety of grain size parameters that are shown graphically as a plot of percentage of volume vs. grain size for each individual sample (Fig. 2). To assess the relative amount and size of inorganic particles in the sediment, 10 samples from the UA-03A core and four samples from the OA-03C core were each split into two subsamples. One split was treated three times with 5% sodium hypochlorite to remove organics, then analyzed with the diffractometer; these analyses provide an estimate of the grain size of the inorganic component of the sediment collected from the Upper and Oaks Arms of the lake. The "inorganic" fraction not dissolved by the sodium hypochlorite includes silicate sediment, the siliceous tests of diatoms, and any detrital carbonate grains derived from the Franciscan formation.

Cores UA-03B, OA-03B, and LA-03B were used for physical description, X-radiography, and magnetic analyses. While still encased in the polyvinyl chloride coring tube, X-radiographs were taken of each core. The cores were then split, photographs of the half-cores were taken, and the images were spliced together using Adobe Photoshop for archival purposes. Low-field volumetric magnetic susceptibility (k) measurements were performed on the split core section using a Bartington point source magnetic susceptibility sensor (Witney,

Oxford, UK) at 1-cm intervals. For additional magnetic measurements, U-channel samples were collected; U-channels are rigid, U-shaped, plastic liners with a 2×2 cm square cross-section and a lid constituting one of the sides. An empty U-channel (without lid) of the same length as the core section was pushed into the split face until the U-channel filled with sediment. The sediment at the base of the U-channel was then cut away with monofilament fishing line, the U-channel extracted, and the lid clipped in place. The ends of the U-channel were sealed with clear polyethylene tape, and the U-channels were refrigerated at 6°C during storage. Magnetic measurements were made after warming to room temperature.

Magnetic measurements were carried out at 1-cm intervals on an automated 2G Enterprises "U-channel" cryogenic magnetometer (2G Enterprises, Mountain View, California, USA). The natural remanent magnetization (NRM) of U-channel samples was measured and then progressive stepwise alternating field (AF) demagnetization was carried out in 5 mT steps to 50 mT. Anhysteretic remanent magnetization (ARM) was then imposed using a 100-mT peak AF and a 0.05-mT direct current (DC) biasing field. The ARM was measured, then remeasured after AF demagnetization at peak fields of 5, 10, 15, 20, 25, 30, 35, 40, 45, and 50 mT.

Information about the concentration and grain size of the magnetic fraction can be constructed from these magnetic parameters (e.g., Thompson and Oldfield 1986). In certain instances the variations in magnetic parameters may reflect primary terrigenous inputs and therefore may be used as sedimentological proxies. However, magnetic parameters are also sensitive to diagenetic changes, which may result in transformations of the signal; thus care must be taken to distinguish between these possibilities. In general, the intensity of the ARM is primarily a function of the concentration of fine ferrimagnetic material (i.e., magnetite, maghemite, greigite). Magnetic susceptibility (k) is also a concentration-dependent parameter, but biased towards coarser grained ferrimagnetic materials; k is also influenced to a lesser degree by paramagnetic (i.e., iron-bearing) clays. The ratio of ARM (after 30mT AF demagnetization) to initial ARM (ARM_{30mT}/ARM) relates the ease or difficulty of sample demagnetization in an AF. Higher values indicate that the sample is harder to demagnetize, whereas lower values indicate easier demagnetization. Assuming a ferrimagnetic mineralogy (e.g., titanomagnetite), then variability in ARM_{30mT}/ARM primarily reflects changes in the grain size of the magnetite fraction.

Subsamples of sediment from cores UA-03A, OA-03A, OA-03C, and LA-03A were gently washed through a brass 0.5-mm screen using tap water to recover any coarse organic debris that might be suitable for radiocarbon dating. The coarse material was inspected under a dissecting microscope with enough small twigs, seeds, and leaves recovered to allow us to date several horizons within each core. Samples were pretreated to remove soluble components by heating them in a dilute solution of NaOH, followed by repeated rinses with deionized water until no discoloration of the rinse water was visible. Samples were prepared for dating at the Lawrence Livermore Laboratory Center for Accelerator Mass Spectrometry (Livermore, California, USA) using standard procedures.

Details of the DDD analyses and ^{210}Pb dating are given in Richerson et al. (2008). Dichlorodiphenyldichloroethane is a pesticide that was used to control an explosive gnat population (Richerson et al. 2008, Suchanek et al. 2008*b*), with peak use occurring in 1954. The resolution of the ^{210}Pb dating is limited by the low atmospheric flux of ^{210}Pb at Clear Lake combined with the high sedimentation rates that, together, reduce the activity of ^{210}Pb in the sediments. The ^{210}Pb dating constrained the position of the 1927 horizon to within ± 3 cm in each core, but without any higher-resolution dates above. Thus the data only permit the calculation of long-term post-1927 sedimentation rates.

Results

Visual inspection of the halved cores reveals an organic-rich, thoroughly bioturbated and homogenized sediment column with a remarkable consistency in sediment texture and color. The X-radiographs provide only minimal extra detail and corroborate the lack of obvious, discernable sedimentary structures and are therefore not reproduced for this paper. In general, the sediments consist of olive green, organic-rich silt and fine sand exhibiting a unimodal distribution. Subtle color changes in two of the cores suggest changing redox conditions. In over-penetrated core OA-03B, olive green colors (3/10Y on a Munsell color chart) are overlain sharply by slightly browner olive green colors (4/5GY) at 63 cm below the top of the core liner. In the longer adjacent core OA-03C, where grain size was actually measured, this horizon projects to 133 cm below the top of the core (Fig. 3D). In core UA-03B, a comparable color change occurs at 78 cm, although the boundary is gradational over a 2–3 cm interval. No apparent redox boundary was recognized in core LA-03B. In both the OA and UA cores, the redox boundary occurs at a depth coincident with the ^{210}Pb-dated 1927 horizon and the associated abrupt changes in TotHg and other chemical parameters (Richerson et al. 2008). The redox boundaries were recognized independently and subsequently shown to correlate with the ^{210}Pb-dated 1927 horizon (Richerson et al. 2008).

Grain size and composition

Fig. 3A–C shows the grain size distributions for the d10, d50, and d90 fractions of the three cores. The d50 value represents the median grain diameter at the midpoint of the grain size distribution, whereas the d10 and d90 fractions represent the grain diameters at the 10 and 90 percentile values along the cumulative curve (Fig. 2). Only 10% of the total grain volume is

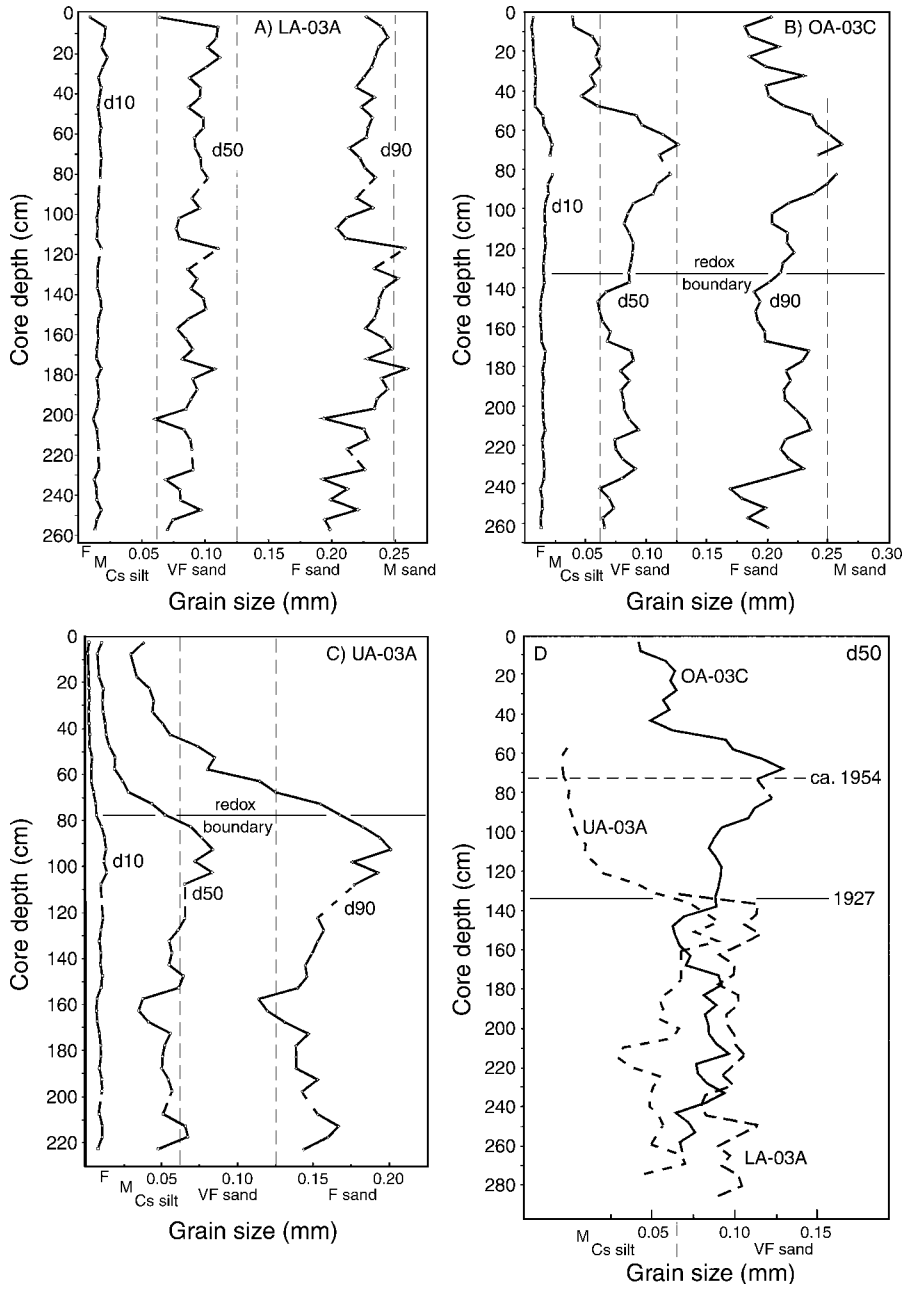

FIG. 3. Stratigraphic distribution of the d10, d50, and d90 grain size fractions from cores (A) LA-03A, (B) OA-03C, and (C) UA-03A. The horizontal lines on (B) and (C) mark the position of the redox boundary that coincides with the 1927 datum. (D) Correlation of stratigraphic patterns of median grain size for the three cores using the 1927 datum and 1954 dichlorodiphenyldichloroethane (DDD) datum. The position of the DDD horizon on core OA-03C was projected from the adjacent core OA-03A. The lower portion of the core LA-03A d50 curve (full data set shown in panel A) has been left off for convenience. Core UA-03A is shown as a short dashed line, and core LA-03A is shown as a long dashed line to distinguish between the plots. The depth axis for all the data is that for core OA-03C. See Fig. 2 legend for key to abbreviations.

finer than the d10 value and only 10% of the total grain volume is coarser than the d90 value.

Core LA-03A mostly exhibits monotonously consistent patterns in grain size throughout the entire 260-cm length of the core except at the very surface; this is because the vast majority of the core represents sediments below the 1927 horizon (Fig. 3A). Median grain size (d50) stays in the range of very fine sand (mean of 0.090 mm) on the Udden-Wentworth grain size scale, whereas the d10 fraction is medium silts (mean of 0.016 mm) and the d90 fraction is fine sands (mean of 0.227 mm). The only significantly different stratigraphic trend in core LA-03A occurs near the top 5 cm where grain size abruptly decreases in all three measured

fractions, which occurs coincident with the 1927 horizon identified in Richerson et al. (2008).

In core OA-03C, median grain size averages 0.078 mm, very fine sand (Fig. 3B). The d10 fraction is composed of fine to medium silt, whereas the d90 fraction is fine sand. A gradual coarsening-upward trend is evident in core OA-03C between 150-cm and 65-cm core depth, with median grain size gradually increasing from a minimum of 0.060 mm (coarsest silt) to a maximum of 0.127 mm (finest fine sand). This upward increase in grain size from 150 to 65 cm is matched in the d90 fraction (reaching the lower limit of medium sand) and subtly in the d10 fraction. From 65 to 40 cm, sediment particle size decreases abruptly with d50 values approaching medium to coarse silts. Above 40 cm, grain size remains relatively constant to the top of the core. The d90 size range fluctuates above 65 cm, but also shows a net decrease toward finer sand between 65 and 40 cm. A subtle size decrease is also evident in the d10 fraction.

In core UA-03A, median grain size averages 0.046 mm (coarse silt), with the average d10 value in the fine to medium silt range and the average d90 value in the very-fine-to-fine sand range (Fig. 3C). A coarsening-upward to fining-upward trend is recognized in core UA-03A above 165 cm. The coarsening-upward trend in the d50 fraction is gradual between 165 and 90 cm, beginning in medium silt and increasing to very fine sand. Above 90 cm, grain size sharply decreases into fine silt near 50–60 cm depths, holding at that size to the top of the core. These stratigraphic patterns are particularly well illustrated in the d90 fraction, where grain sizes range from fine sand at the coarsest (90 cm) to medium silts at the top of the core. The d10 fraction exhibits the same upward trends when particle size is plotted (not shown) on a log scale.

Using the 1927 datum established by ^{210}Pb dating (Richerson et al. 2008) in connection with the known history of Hg mining in the watershed (Suchanek et al. 2003, 2008*b*), the median grain size plots from the three cores were correlated to assess temporal trends (Fig. 3D). An accessory date used for correlation and interpretation is provided by DDD profiles within the UA-03A and OA-03C cores (Richerson et al. 2008). Median grain size in core UA-03A (medium to coarse silt) is significantly finer than in the other two cores (very fine sand). Furthermore, above the 1927 datum, median grain size exhibits a sharp fining-upward pattern in UA-03A, whereas in OA-03C a gradual coarsening-upward trend evolves into a fining-upward pattern. It is apparent from Fig. 3D that most of the post-1927 sediment in the LA-03 core is missing. Possible reasons for this include over-penetration during coring, non-deposition at this location, or removal of sediment by subaqueous erosion, either natural or human-induced.

The grain size trends discussed above are based on sediment samples comprised of both inorganic and organic particles. The Clear Lake sediments contain abundant organic matter. The inorganic content of the cores is generally between 15% and 25% on a dry-mass basis (Richerson et al. 2008) and form an even smaller fraction on a volume basis. In Clear Lake, inorganic grains may include silicate grains derived from the source terrain in the watershed, siliceous diatom tests not dissolved by our washing technique, and any carbonate grains derived from the Franciscan bedrock. Organic particles may be derived from biogenic processes within the lake as well as from the watershed, thus organic matter may be both authochthonous and allochthonous. Examples range from the remains of cyanobacterial blooms to woody plant debris washed in through streams.

The results of our experiment on 10 samples from the Upper Arm core that separated the inorganic fraction from the combined sediment reveal two general patterns (Fig. 4). First, the actual size of inorganic particles is significantly finer than the untreated, combined sediment. This suggests that the median and coarse fractions of the combined sediment are dominated by organic particles that range in size from medium silt (d50) to fine sand (d90). In contrast, the inorganic grains range in size from fine silt (d50) to coarse silt/very fine sand (d90). Second, the grain size trends of the finer, inorganic particles parallel those of the combined sediment in both the d50 and d90 fractions. In the d90 fraction above ~140 cm, the inorganic particles coarsen to ~90 cm, then fine upward to the top, similar to the combined sediment. In the d50 fraction, both the inorganic and total sediment exhibit a fining-upward pattern above ~90 cm. These coincident stratigraphic trends in both size fractions suggest that, in the Upper Arm, both organic and inorganic particles responded in a like manner to changing depositional conditions. Even though this separation experiment involves a small number of samples, we believe the patterns revealed about sediment composition, the relative size of inorganic vs. organic particles, and long-term stratigraphic trends are applicable through all three arms of Clear Lake.

Examination of sediment by SEM also suggests a change in sediment character above and below the 1927 horizon. Samples from above the 1927 horizon typically show amorphous texture of organic debris and clay with relatively lower proportion of clean, well-preserved diatom fragments (Fig. 5A, B). Samples from below the 1927 horizon typically show abundant diatom fragments (Fig. 5C, D). This may represent a change in the lake ecology from relatively clearer water dominated by aquatic plants and diatoms prior to anthropogenic disturbance to a cyanobacterial-dominated ecosystem, as occurs at present, in response to anthropogenic changes in nutrient loading and diagenetic cycling.

Magnetic properties

In Fig. 6, three different magnetic parameters (k, ARM, and ARM_{30mT}/ARM) are plotted for each core. Across each row of data are the results for cores UA-

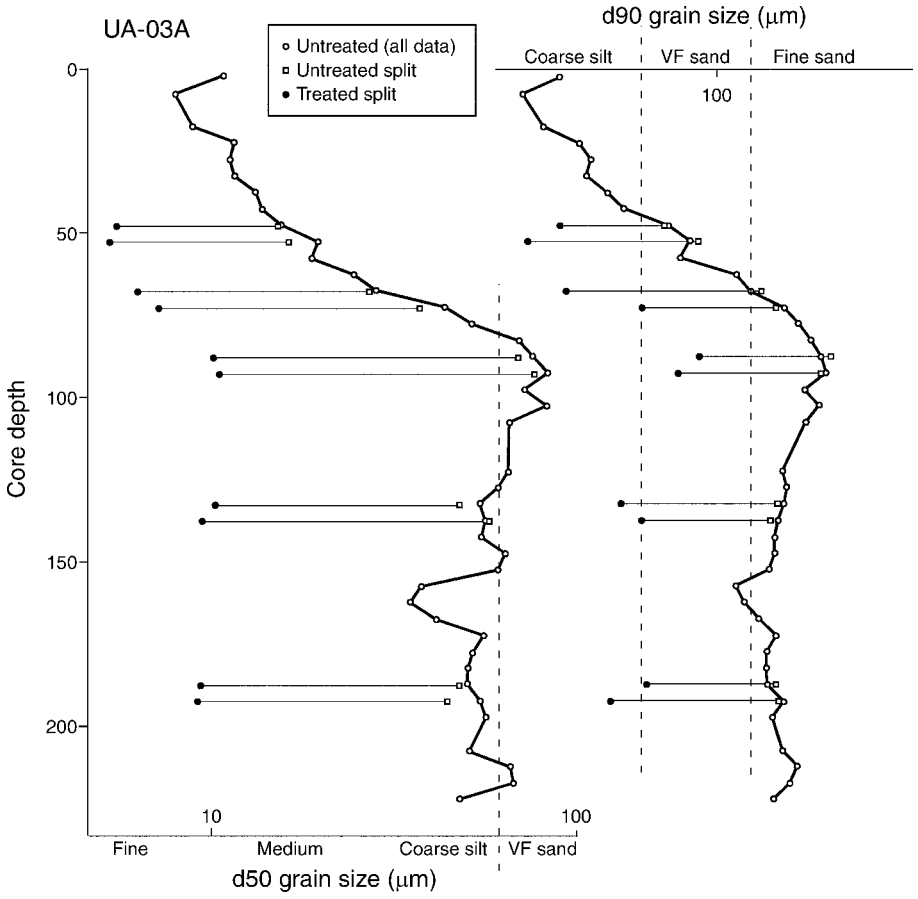

FIG. 4. Stratigraphic distribution of the 10 treated (small solid circles) and untreated (open squares) samples of the d50 and d90 fractions from core UA-03A, plotted alongside all grain size data (connected open circles; "VF" stands for very fine). The horizontal scales are the natural logarithm of grain size in micrometers. See Fig. 2 for a definition of fractions. The vertical dashed lines mark the boundaries between the grain size cutoffs on the horizontal axes. On the left side, the dashed line separates coarse silt from VF sand, whereas on the right side, the dashed lines separate coarse silt from VF sand from fine sand.

03B, OA-03B, and LA-03B, with all depth records correlated relative to the 1927 datum in the far right panels. Overall, the low coercivity magnetic behavior and its demagnetization characteristics are consistent with a dominantly ferrimagnetic (e.g., titanomagnetite) mineralogy derived from detrital sources, though the presence of other magnetic minerals cannot be completely ruled out. Core UA-03B has higher values of k, ARM, and ARM_{30mT}/ARM above the 1927 datum, indicating higher magnetic concentrations from k and ARM and finer magnetic grain size from ARM_{30mT}/ARM. Below the 1927 datum, concentrations of magnetic minerals are significantly reduced in all cores, though differences in concentration between UA-03B and OA-03B as indicated by ARM are almost one order of magnitude, with LA-03B falling in between (Fig. 6B). Though a much less sensitive measurement at these low concentrations, k shows a similar relationship between cores. Grain size differences in the magnetic carrier indicated by ARM_{30mT}/ARM also show the same relationship with UA-03B having the finest and OA-03B having the coarsest, consistent with the grain size distribution of all sediment from the lake (Fig. 3D). Therefore the relationship between cores and the transition down-core are similar with the highest magnetic concentrations associated with the finest magnetic grain sizes and vice versa. This relationship and the transition from higher concentrations and finer grain sizes above the 1927 horizon to lower concentrations and coarser grain sizes beneath is consistent with and characteristic of titanomagnetite dissolution. Magnetic dissolution results in a magnetic assemblage of decreased concentration and increased magnetic particle size (e.g., Karlin and Levi 1983).

Radiocarbon age corrections

Results of the AMS dating on ^{14}C of coarse organic debris are presented in Table 1 as radiocarbon years ($\pm 1\sigma$) and as age ranges in calendar years before present (ybp), after correction for reservoir dead carbon incorporation and calibration for variations in the production rate of ^{14}C (explained below in *Discussion*). Fig. 7 shows the stratigraphic position of the calibrated

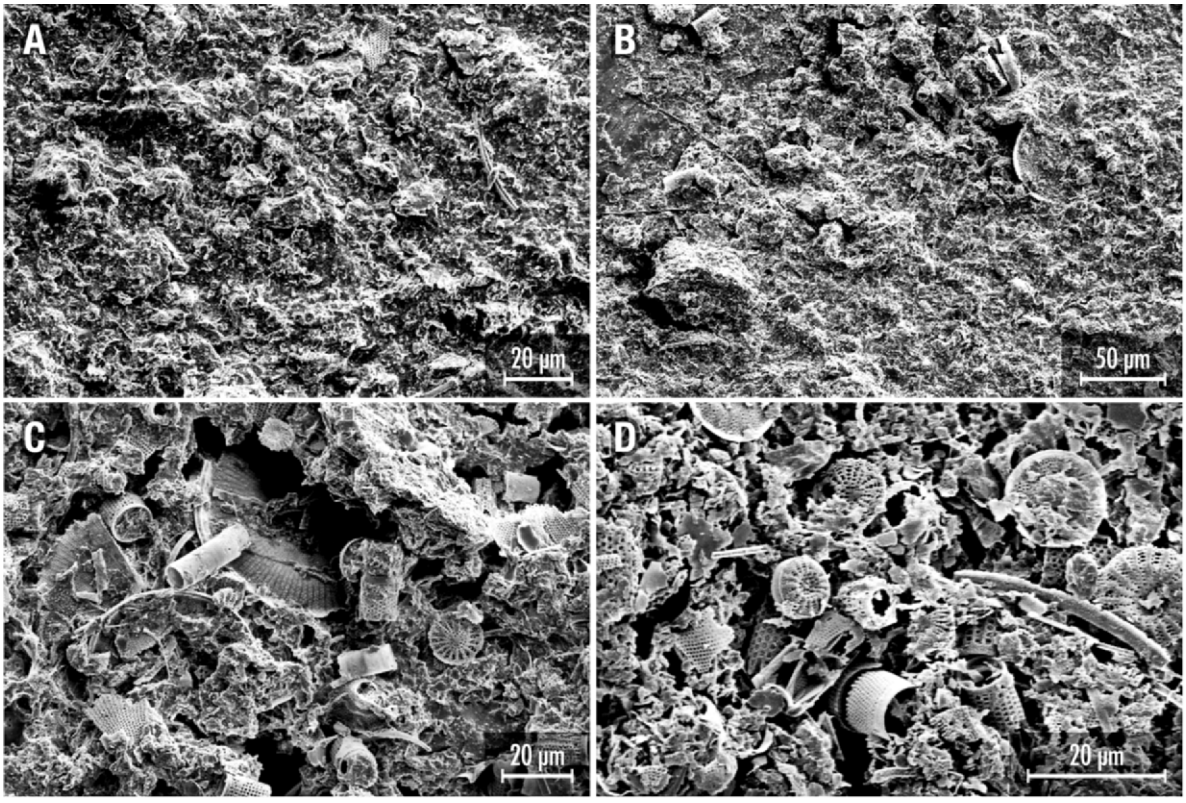

FIG. 5. Secondary electron scanning electron microscope images contrasting the nature of pre- and post-anthropogenic changes in the sedimentation regime of the Upper Arm. (A) Near-surface sediment representative of the present conditions in Clear Lake, which are dominated by summer blooms of cyanobacteria (core UA-03A, 0–5 cm depth). (B) Shallowly buried sediment above the 1927 horizon is similar to surface sediment (core UA-03A, 15–20 cm depth). Sediment below the 1927 horizon (78 cm depth) tends to show a greater abundance of diatom fragments. (C) Core UA-03A, 120–125 cm. (D) Core UA-03A, 155–160 cm.

radiocarbon dates for three cores plotted against median grain size. All of the dates are consistent with stratigraphic position with the exception of the sample from OA-03C (140–145 cm), which we interpret to be older organic material redeposited into younger sediment. This sample is not considered in subsequent discussions.

The Clear Lake area is an active volcanic province with abundant discharge of ^{14}C-free CO_2 in hot spring fluids and gas vents (Bergfeld et al. 2001). The dominant source of CO_2 is from metamorphic calcite veins and organic carbon in the Cretaceous age Franciscan Formation shale and greywacke (Bergfeld et al. 2001). Carbon dioxide venting from the Sulphur Bank geothermal system may also have a small component of magmatic carbon (Bergfeld et al. 2001). Venting of geothermally derived CO_2 directly into the lake results in ^{14}C values for organic matter that yield anomalously old ^{14}C ages due to incorporation of "dead carbon." Previous studies showed that ^{14}C ages on Clear Lake sedimentary bulk organic matter had to be corrected by 4200 years to obtain reasonable sedimentation ages (Robinson et al. 1988). In an attempt to avoid this problem, we selected coarse, terrigenous organic debris washed into the lake for dating, with the recognition that the terrigenous plant debris may have some storage time before entering the sediment and that the potential for reworking of older organic debris into younger sediment could occur. The amount of sample material was generally too small to allow for $\delta^{13}C$ measurements so samples were corrected for carbon isotope fractionation assuming a $\delta^{13}C$ value of 25‰. Two samples were run for $\delta^{13}C$ and gave values of −26.9‰ and −28.8‰ (OA-03A 275–280 cm and OA-03C 255–260 cm, respectively).

Comparison of the ^{14}C dates in sediments near and above the 1927 horizon with ^{210}Pb dates indicates that the plant materials give dates in ^{14}C years that are ~300 years too old, which is interpreted to reflect the incorporation of volcanically derived dead carbon into the woody debris dates. This magnitude of correction is equivalent to incorporation of 3.4% volcanically derived dead carbon into the organic matter at the time of plant growth. Such effects have been seen in other areas where geothermal discharge releases radiocarbon-depleted CO_2 into the shallow groundwater and/or atmosphere (Pasquier-Cardin et al. 1999). For example, venting of CO_2 in the Mammoth Lakes, California, area has

resulted in plant material that can contain in excess of 85% volcanically derived, radiocarbon-free carbon (Cook et al. 2001).

The AMS ^{14}C dates for samples below the 1927 horizon were corrected for dead carbon incorporation by assuming that the ^{210}Pb date for this horizon of 1927 is accurate. A linear regression of the AMS ^{14}C dates vs. depth below the 1927 horizon (assuming constant sedimentation rates) gives a ^{14}C age of 360 years for this horizon (Fig. 8), compared to the expected ^{14}C age of 23 years (1950–1927). (Zero years before present, 0 ybp, equals AD 1950; [Stuiver et al. 2005].) The difference in age (337 years) is inferred to be the average reservoir correction, which includes both the incorporation of geothermally derived dead carbon and the transport time required to deposit coarse organic material in the sediment. The AMS ^{14}C dates for samples deposited below the 1927 horizon were corrected for dead carbon by subtracting 337 years, and the resulting ages were then calibrated for changes in ^{14}C production rate using the program CALIB. version 5.02 (Stuiver et al. 2005). The corrected and calibrated ages are presented in Table 1.

Samples collected above the 1927 horizon cannot be corrected in the same manner because the sedimentation rates change across the 1927 horizon. It is interesting to note that if we assume that the same reservoir correction is appropriate for sample UA-03A (70–75 cm), collected 5.5 cm above the 1927 horizon, we calculate a ^{14}C age of 33 years (1917). Given the ± 50 year counting errors for this sample, the corrected age is consistent with the stratigraphic position of the sample. However, applying the same correction to sample OA-03C (110–115 cm) collected 20.5 cm above the 1927 datum results in a negative age for this sample, yielding a calendar age of 1997 $\pm$ 40 yr. Samples UA-03A (0–5 cm) and OA-03C (30–35 cm) both contain excess ^{14}C indicative of formation after the rise in radiocarbon due to atmospheric testing of nuclear weapons. The concentration of ^{14}C in these samples suggests that OA-03C (30–35 cm) must have formed early in the rise of bomb ^{14}C during the mid- to late 1950s while UA-03A (0–5 cm) is consistent with formation either in the late 1950s to early 1960s or in the mid- to late 1980s (T. Guilderson, *personal communication* 2001). Based on the stratigraphic position of sample UA-03A (0–5 cm), we interpret that it formed in the late 1980s.

Pre-anthropogenic sedimentation rates

Pre-1927 sedimentation rates were determined by linear regression of the corrected and calibrated ^{14}C dates vs. depth below the 1927 horizon (Fig. 8). A linear fit of the data between ~1400 ybp and the 1927 datum ($R^2 = 0.922$) yields a sedimentation rate of 1.0 mm/yr for each of the arms of the lake and passes near zero age at the 1927 horizon. At a depth of ~140 cm below the 1927 horizon (~1400 ybp), the sedimentation rates for the Lower Arm appear to diverge from the rest of the lake. Age vs. depth for these deeper samples gives sedimentation rates of 0.63 mm/yr ($R^2 = 0.98$) for the Upper Arm and Oaks Arm and 2.0 mm/yr ($R^2 = 0.91$) for the Lower Arm.

Long-term sedimentation rates in Clear Lake were determined previously from radiocarbon dates of the upper 40 m of long cores (115 and 169 m) collected by Sims et al. (1988) and integrated with regionally correlative tephra units. After correction for both reservoir and "old carbon" effects (Robinson et al. 1988), they arrived at rates of 0.4 to 0.9 mm/yr for the past 0.45 million years (my) with a possible overall rate of 1.7 mm/yr over the past 0.6 my (Hearn et al. 1988). These rates are comparable to those calculated from the pre-1927 ^{14}C data in this study.

Discussion

Pre-1927 sedimentation

The divergence in sedimentation rates between the Lower Arm and the Upper and Oaks Arms prior to ~1400 ybp suggests a major reorganization in the drainage patterns or the hydrology of Clear Lake. Given the active tectonic and volcanic setting of the area, it is not surprising that sedimentation patterns in the lake could shift quickly. Enhanced stream input into the Lower Arm prior to ~1400 ybp could account for the doubling of the sedimentation rate, but morphological evidence for a major drainage input is not apparent. Alternatively, a catastrophic event, such as a landslide or sector collapse from the Mt. Konocti volcano could have formed a sill, partially separating the Lower Arm from the rest of the lake and restricting the delivery of sediment. Another possibility is that a reorganization of the drainage outlet in the Lower Arm, perhaps in response to tectonic activity, could have changed lake circulation and sedimentation.

Synchronicity of trends

Using the 1927 datum, we correlated median grain size, percentage of dry mass, ARM_{30mT}/ARM (a measure of magnetic grain size), and TotHg for the three cores (and their pairs) in this study (Fig. 9). The redox boundaries recognized visually as color changes in the UA-03 and OA-03 cores coincide with the 1927 datum and associated abrupt shifts in all four parameters. Below the 1927 datum, all three cores record relatively consistent characteristics. Median grain size doesn't change appreciably, holding relatively constant with only a few minor perturbations. Percentage of dry mass gradually increases downward from the datum, reflecting the progressive loss of pore water with depth due to compactional dewatering. The ARM_{30mT}/ARM ratio remains relatively stable below the 1927 datum, and total Hg remains relatively constant (other than small spikes low in the OA-03 and UA-03 cores).

Above the 1927 datum, however, all four parameters show significant shifts from the pre-1927 background levels (Fig. 9). Median grain size in core UA-03 abruptly

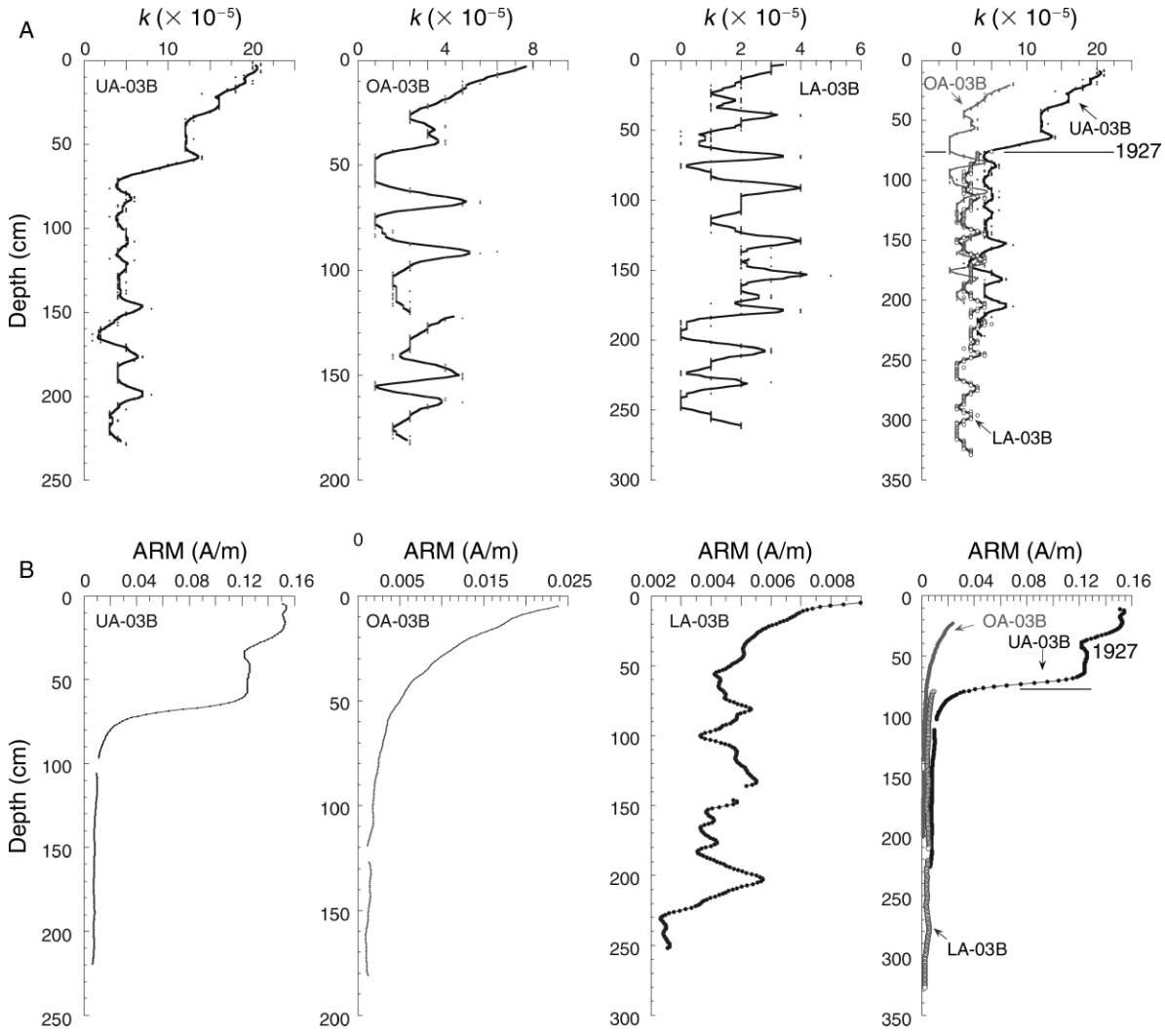

FIG. 6. Comparative plots of (A) k, (B) ARM, and (C) ARM_{30mT}/ARM for cores UA-03B, OA-03B, and LA-03B. The parameter k is a dimensionless measure of magnetic susceptibility in SI units, whereas ARM is the anhysteretic remanent magnetization (in amps per meter). The ratio of ARM_{30mT} (after demagnetization) to initial ARM relates the ease or difficulty of sample demagnetization in an alternating field and is a measure of grain size of the magnetic fraction.

decreases above the datum before stabilizing in the upper 40 cm. In contrast, d50 values above the datum in OA-03 show a gradual coarsening-upward to a fining-upward pattern. Median grain size in LA-03 appears to abruptly fine above the 1927 datum (at least for one data point). Percentage of dry mass in UA-03 and OA-03 increases then decreases, recording progressively lower water content above the 1927 datum, followed by a return to wetter sediments toward the top of each core. The ARM_{30mT}/ARM ratio in UA-03 and OA-03 exhibits abrupt increases, suggesting finer magnetic grain sizes post-1927. The magnetic transition in LA-03 occurs only in the topmost few centimeters and is much more subtle than in the other two cores. The sharp increase of TotHg to concentrations two to nine times pre-1927 levels has been well documented (e.g., Suchanek et al. 1997, Richerson et al. 2000, 2008). Decreases in C, N, and S concentration occur beginning at the 1927 horizon due to increased sedimentation rate and dilution by inorganic matter (Richerson et al. 2000, 2008). Despite the decreases in concentration, calculated mass accumulation rates (in milligrams per square centimeter per year) for C, N, and S exhibit an increase of one order of magnitude after 1927 (Richerson et al. 2008). Clearly, environmental conditions in the Clear Lake watershed changed in a significant fashion in the 1920s (Richerson et al. 1994, 2000, Suchanek et al. 2003). The following sections discuss the diagenetic and anthropogenic controls on the post-1927 synchronous changes in particle size, magnetic properties, and redox conditions in the Clear Lake cores.

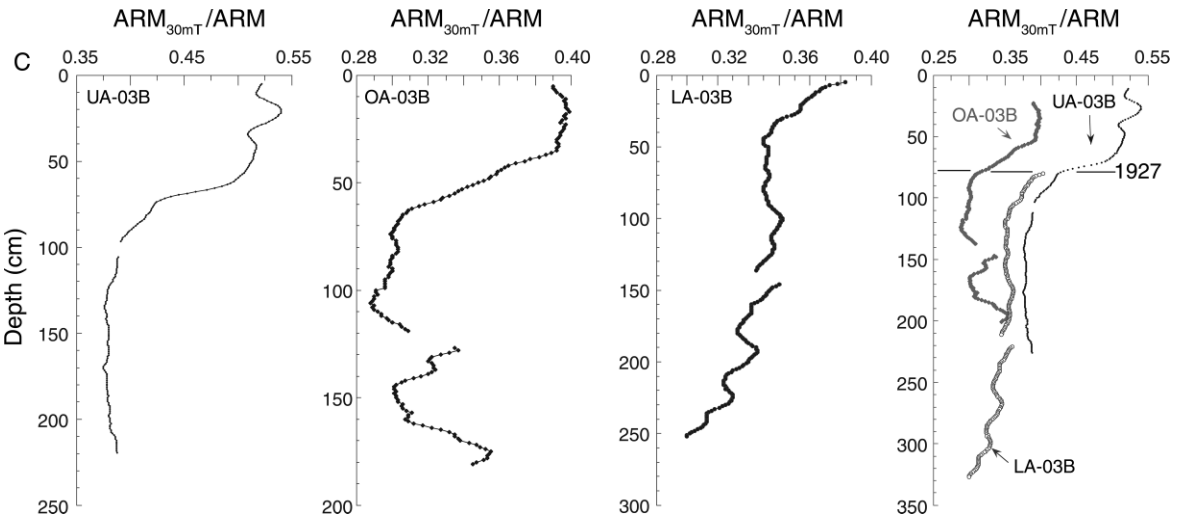

FIG. 6. Continued.

Reduction diagenesis

Depositional evidence for an abrupt increase in sedimentation rate post-1927 is provided in cores OA-03C and UA-03 by the co-occurrence of abrupt shifts in magnetic signatures with color differences indicative of changing redox conditions. Magnetic concentrations increase significantly above the 1927 datum (Fig. 6A), accompanied by a sharp transition to finer magnetic grain sizes (Fig. 6C). The coincidence of the 1927 horizon with a color change in the sediment from darker olive green sediment below to lighter, more brownish sediment above suggests a change in diagenesis to relatively more oxidizing conditions above the 1927 horizon (Fig. 9). The change in the diagenetic regime is likely related to the observed increase in sediment accumulation rate at this boundary. The organic-rich sediments of Clear Lake have excess reducing capacity and the microbial breakdown of organic matter is limited by presence of electron acceptors.

Sulfate reduction is active at very shallow depths in the sediment (Mack 1998, Shipp and Zierenberg 2008). With the exception of areas close to the mine affected by

TABLE 1. Results of the accelerator mass spectrometry (AMS) ^{14}C dating of coarse organic debris from four cores from Clear Lake, California, USA.

Sample number	Core	Depth (cm)	^{14}C (yr)	Calibrated age range (1σ), ybp	ybp	ybp rounded	Absolute date
77744	UA-03	0–5	modern		modern		
77743	UA-03	70–75	370 ± 50	33–73	uncalibrated		
77742	UA-03	140–145	1040 ± 140	541–744	669	670	1330
77741	UA-03	190–195	1400 ± 70	924–1058	983	980	1020
76003	UA-03	225–227	2180 ± 40	1724–1822	1779	1780	220
76002	UA-03	225–227	2270 ± 50	1823–1932	1881	1880	120
77733	OA-03A	65–70	440 ± 40	56–138	116	120	
77734	OA-03A	95–100	660 ± 50	349–439	391	390	1610
77739	OA-03A	155–160	1150 ± 40	685–743	725	730	1270
77740	OA-03A	190–195	1760 ± 50	1293–1356	1330	1330	670
76005	OA-03A	275–280	2940 ± 50	2707–2779	2734	2730	730 BC
76004	OA-03A	275–280	3030 ± 50	2757–2807	2805	2800	800 BC
77748	OA-03C	30–35	modern		modern		
77735	OA-03C	110–115	290 ± 40		uncalibrated		
77736	OA-03C	140–145	1660 ± 40	1255–1295	1257		
77737	OA-03C	205–210	1000 ± 40	639–668	621	620	1380
76006	OA-03C	255–260	1830 ± 50	1315–1412	1381	1380	620
77745	LA-03	35–40	600 ± 60	350–436	318	320	1680
77746	LA-03	100–105	1160 ± 40	690–745	734	730	1270
77738	LA-03	155–160	1830 ± 50	1315–1412	1381	1380	620
77747	LA-03	200–205	2130 ± 50	1692–1814	1722	1720	280
76001	LA-03	260–265	2260 ± 50	1819–1929	1870	1870	130

Notes: Included are the raw data in radiocarbon years, 1σ calibrated age ranges, an estimated single age (in years before present [ybp], from year 2000) based on the median probability, the rounded age (ybp) based on recommendations in Stuiver et al. (2005), and the absolute date (AD/BC). Calibration was done using Calib. 5.02 (Stuiver et al. 2005), which also provided the single median probability age. The median probability by itself does not represent the calendar age of the sample, but rather simply provides a value that can be plotted to estimate sedimentation rates from the calibrated data (Fig. 8).

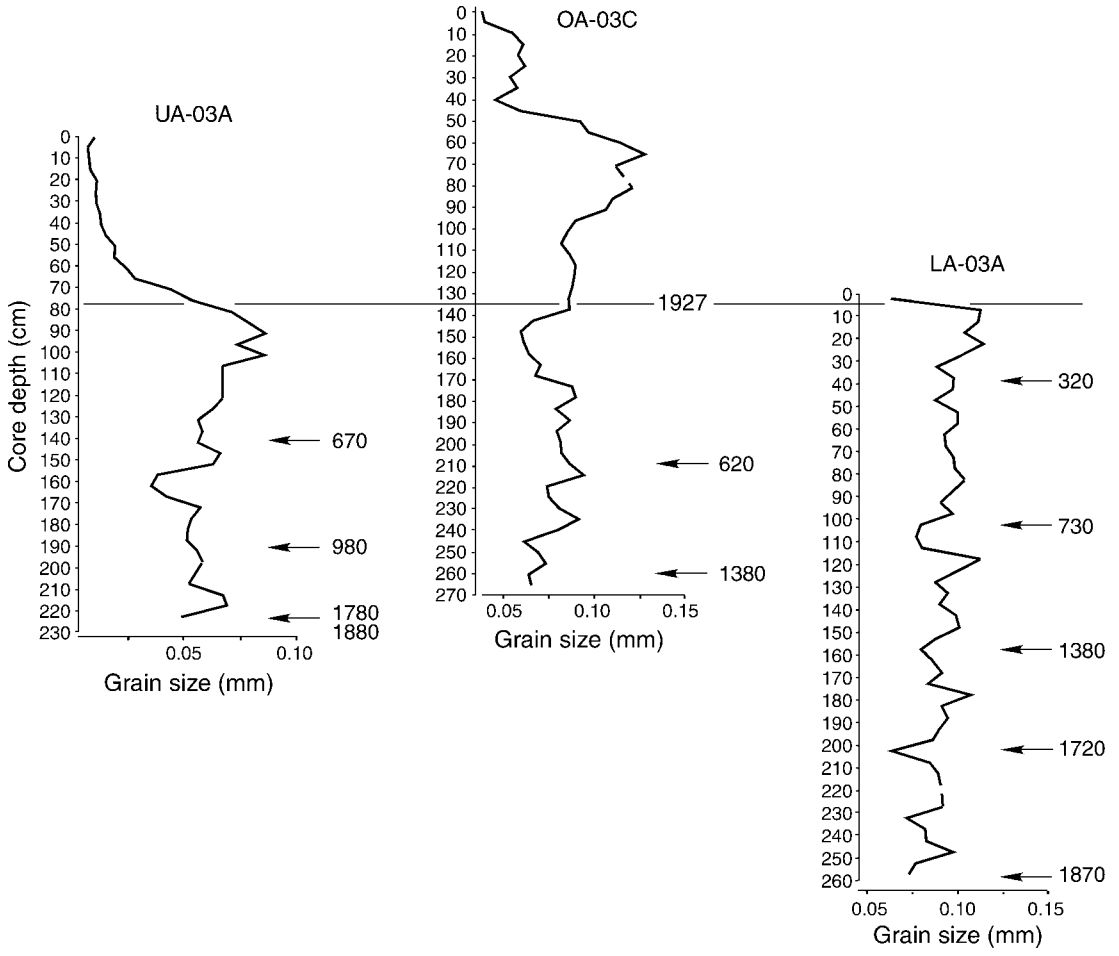

FIG. 7. Stratigraphic position of calibrated radiocarbon dates (values at arrows in years before present) vs. median grain size for cores UA-03A, OA-03C, and LA-03A (data from Table 1). The relative order of dates is consistent with depth in the cores. Radiocarbon dates for core OA-03A are not shown because no grain size measurements were made on that core, but the ^{14}C ages are consistent with stratigraphic position as in the other cores (see Richerson et al. 2008). "Modern" dates and uncalibrated dates above the 1927 horizon are not shown.

subsurface flow of sulfate-rich acid mine drainage, the amount of anaerobic oxidation of organic matter is limited by the availability of sulfate. Sulfate is totally depleted by bacterial sulfate reduction at sediment depths greater than ~15 cm (Shipp and Zierenberg 2008). Sulfur isotope values of diagenetic pyrite in a core collected away from the mine also indicate quantitative closed system reduction of sulfate to sulfide in the lake sediments (Shipp and Zierenberg 2008). The amount of reduced sulfur fixed in the sediment is not limited by the availability of organic carbon, but rather by the availability of either sulfate or iron. Acid mine drainage from the abandoned mine is a significant source of sulfate to Clear Lake (Richerson et al. 2008, Shipp and Zierenberg 2008). Historic data on the sulfate concentration of Clear Lake are not available, but it seems likely that sulfate added to Clear Lake by acid mine drainage has increased the sulfate content of the lake. We hypothesize that higher sulfate concentrations result in increasing the depth to which sulfate can diffuse into the lake sediments, with the result that the bacterial sulfate reduction zone now extends to greater depths in the sediment. Alternatively, the increased sulfate could simply enhance the activity of sulfate-reducing bacteria. In either case the result would be an increase in the oxidation of organic carbon in response to the increased sulfate load. This change has likely been responsible for the post-1927 change in diagenetic regime, which has resulted in relatively more oxidized sediments that have lower preservation of organic material despite increases in the sedimentation rate and C loading (Richerson et al. 2008). Iron cycling is also affected by these changes as reflected in the changing magnetic properties of the cores.

Sulfur content of sediments deposited below the 1927 horizon ranges from 0.4% to 0.8% in the Upper Arm and is typically between 1% and 1.5% in the Lower Arm and Oaks Arm (Richerson et al. 2008). The low values of magnetic intensity below this boundary suggest that

sulfide accumulation in this portion of the cores is iron limited. The presence of sulfide derived by bacterial sulfate reduction has been closely correlated with the diagenetic changes in iron mineralogy in marine sediments (e.g., Bleil 2000, Channell and Stoner 2002). Diagenetic remobilization of iron is reflected in the magnetic properties of the sediment (Karlin and Levi 1983). At high sulfide concentrations magnetite is overgrown and eventually replaced by pyrite, whereas at lower concentrations magnetite undergoes progressive dissolution (Canfield and Berner 1987).

The low intensity of magnetization and the coarser magnetic grain size below the 1927 horizon indicate that diagenetic destruction of fine-grained magnetite in these more slowly deposited, more reduced sediments was essentially syndepositional and that the availability of iron from the detrital magnetite was probably the limiting factor on the accumulation of diagenetic pyrite in these sediments. The amount of dissolved sulfate in the lake water prior to 1927 was likely lower than the present levels as this preceded the flux of acid mine drainage to the lake. This, combined with the more reduced nature of the sediment, suggests that the depth of diffusional penetration of sulfate into the sediment was likely more shallow than at present. Despite these limits, the diagenetic destruction of magnetite was essentially quantitative. The slower depositional rate for these deeper sediments resulted in longer times spent near the sediment/water interface where diffusion of sulfate could support bacterial sulfate reduction and dissolution of iron oxides.

The increase of approximately one order of magnitude in sedimentation rate post-1927 led to burial of sediment below the depth of sulfate diffusion more rapidly than magnetite could be dissolved. The up-core increase in magnetic intensity above the 1927 horizon suggests that magnetite dissolution is ongoing, but unable to keep up with magnetite deposition in the younger sediments with higher accumulation rate. The down-core trend to lower concentrations and coarser magnetic particles with depth is the characteristic signal of magnetite dissolution (Bleil 2000), which preferentially removes the smaller particles that have the highest surface area : volume ratios. Prior to 1927, the diagenetically driven magnetic transition probably occurred over a depth of a few centimeters. The much greater depth of the transition observed here is most likely a relict of the prior conditions trapped by the large influx of sediment post-1927.

The present accumulation of pyrite in the sediments appears to be limited by availability of readily reactive iron. Highly reactive amorphous iron oxyhydroxides are only present in the surface sediments and are quickly reduced to ferrous iron upon burial into the organic-rich sediments. Dissolved ferrous iron in the zone undergoing rapid sulfate reduction is quickly immobilized as iron sulfide. When sulfide production exceeds the availability of readily soluble iron, pyrite can form at

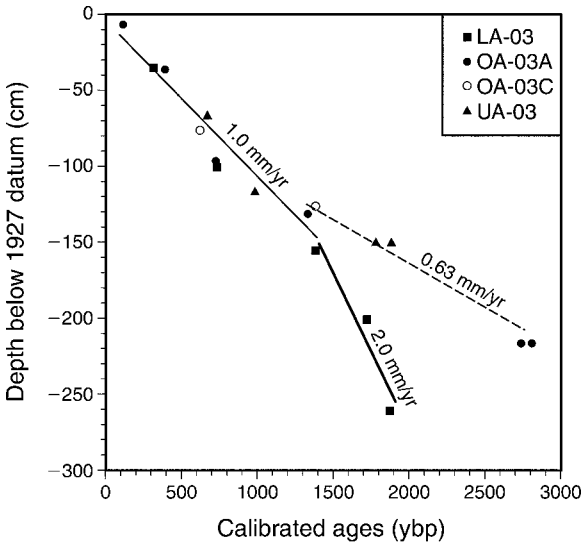

FIG. 8. Plot of depth vs. calibrated ages below 1927 datum (ybp, years before present) used to calculate sedimentation rates. Zero on the vertical axis corresponds to the depth in each core of the 1927 datum, with corresponding dates in ybp derived from the median probability age shown in Table 1.

the expense of detrital magnetite, but the rate at which crystalline magnetite releases its iron is slow compared to amorphous ferric oxyhydroxides. Prior to 1927, the rate at which magnetite could react to form pyrite was fast enough relative to the sedimentation rate and the time to burial below the zone where sulfate diffusion is lower than bacterial sulfate reduction so that magnetite was essentially removed from the sediment in the zone of active diagenesis.

The increase in sediment loading, starting at ca. 1927, changed the diagenetic regime as well. The higher magnetic concentration and finer magnetic grain sizes in the post-1927 sediment are a reflection of the inability of reductive magnetite dissolution to keep up with the increased terrigenous supply. It may seem contradictory that the amount of pyrite sequestered in the sediment, as reflected in the drop in sulfur contents of the cores above the 1927 horizon (Richerson et al. 2008), decreases at a time when anthropogenic loading of sulfate to the lake through acid mine drainage, and perhaps through sulfur additions from agricultural applications, is expected to increase. The increased sulfate should increase the potential for sulfate reduction as well as increase the depth interval over which sulfate can be supplied to sulfate-reducing bacteria by diffusion from the overlying lake waters. This is, in fact, the case. Although the mass percentage of sulfur in the uppermost sediments drops by about a factor of two in the post-1927 deposits due to dilution by increased inorganic sediment input, the mass accumulation rate of sulfur shows a fivefold increase across this boundary (pre-1927 average 0.17 mg $S \cdot cm^{-2} \cdot yr^{-1}$ vs. 0.92 mg $S \cdot cm^{-2} \cdot yr^{-1}$ post-1927; Richerson et al. 2008). Therefore organic diagenesis by

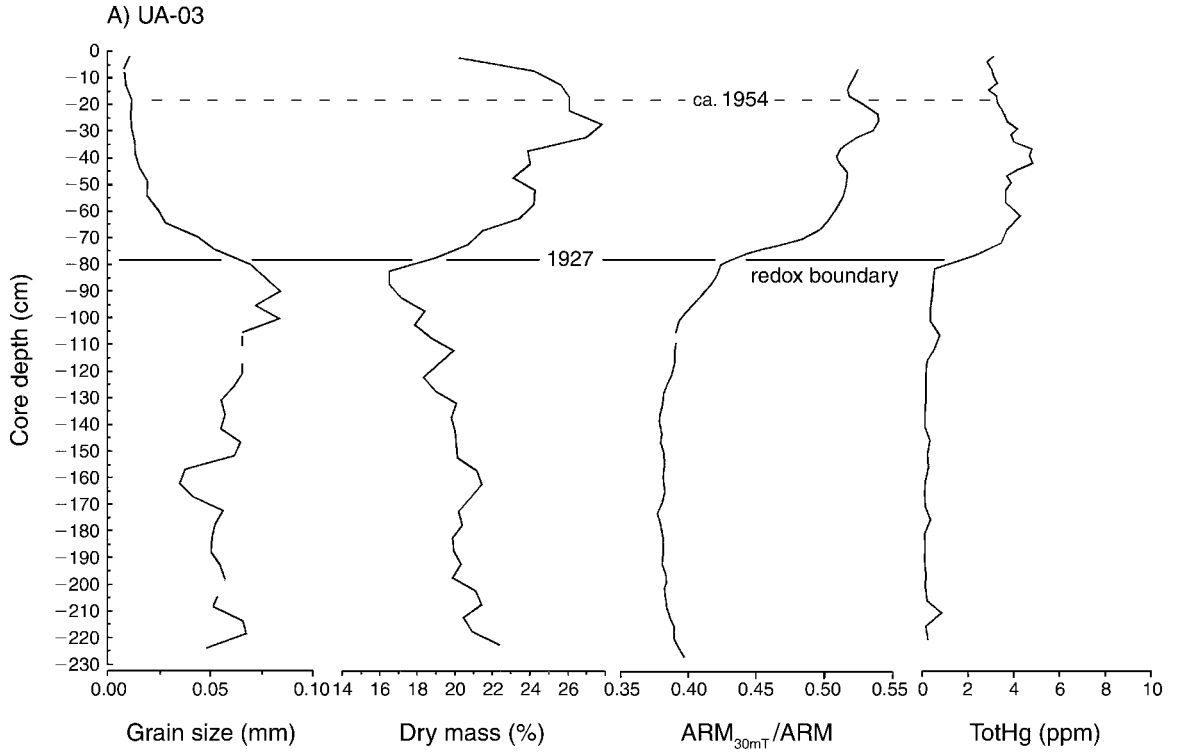
A) UA-03
Core depth (cm)
ca. 1954
1927
redox boundary
Grain size (mm)
Dry mass (%)
ARM30mT/ARM
TotHg (ppm)

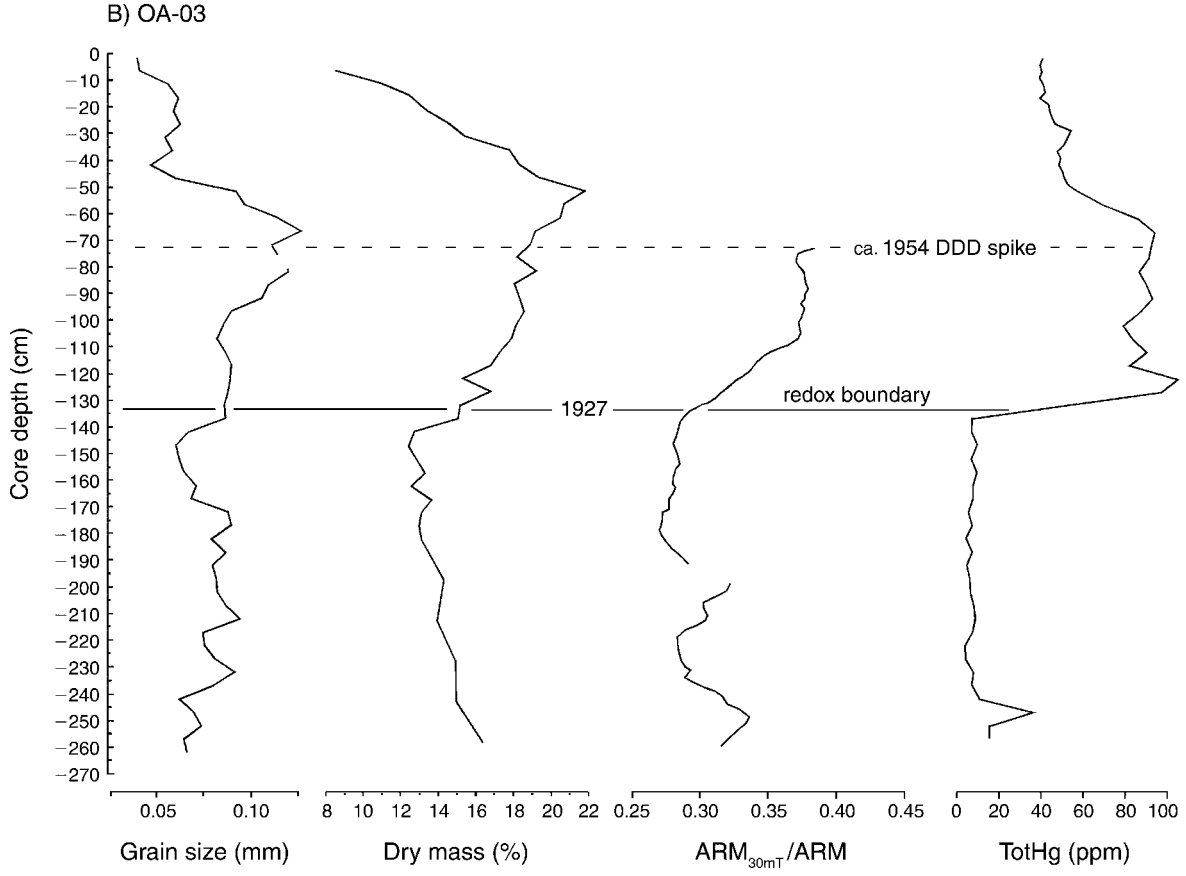
B) OA-03
Core depth (cm)
ca. 1954 DDD spike
1927
redox boundary
Grain size (mm)
Dry mass (%)
ARM30mT/ARM
TotHg (ppm)

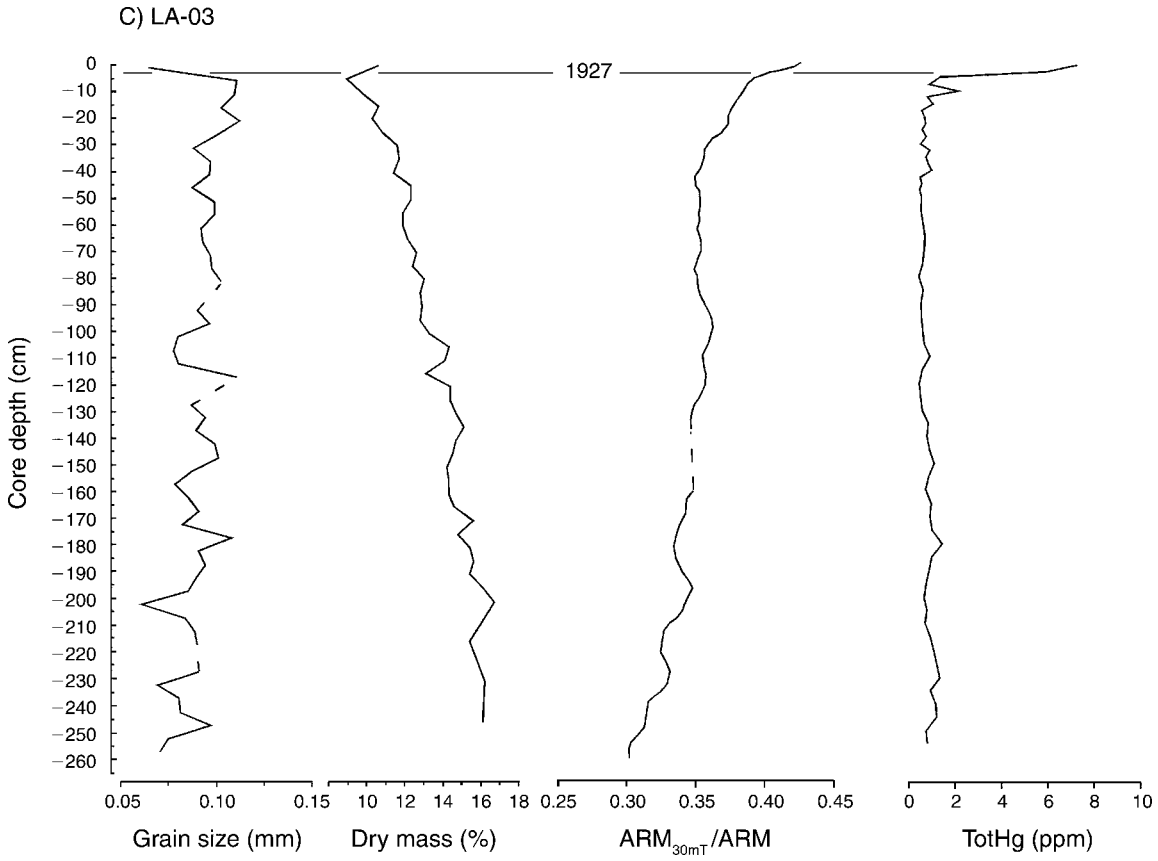

FIG. 9. Continued.

anaerobic sulfate reduction is quantitatively more important in the lake than in the pre-anthropogenic period.

The human-induced increase in sedimentation rate and anthropogenic addition of sulfate to Clear Lake have clearly changed the diagenetic cycling of iron, as indicated by the magnetic properties. These changes have implications for the transport and bioavailability of nutrients, particularly phosphorous, and potentially toxic trace metals, such as Hg, As, and Cu, that can sorb to iron oxyhydroxide phases (Kim 2003). Deepening of the zone of sulfate penetration into the sediments results in a greater separation between the reductive dissolution of amorphous oxyhydroxide phases and the production of hydrogen sulfide that can precipitate and potentially sequester ferrous hydroxide in the sediments. Iron sulfide formed near the sediment–water interface is more likely to undergo repeated oxidation/reduction cycling due to sediment disturbance by currents or bioturbation. Iron sulfide formed deeper in the sediment is more likely to transform to pyrite and be permanently sequestered in the sediments. Because phosphorous cycling is closely tied to iron cycling in lakes, changes in the diagenetic regime can be reflected in changes in the ecology of photosynthetic organisms.

Post-1927 anthropogenic effects on deposition

Oaks Arm.—The initial increase in grain size above the 1927 datum in the OA-03C core (Figs. 3D and 9) is attributed to open-pit mining activities at the mine. Several thousand megagrams of coarse, mechanically mined waste rock were piled up along the shoreline of the eastern tip of the Oaks Arm, extending the shoreline ~100 m into the lake (Chamberlin et al. 1990). The waste rock piles reached heights of 10 m and sloped into the

←

FIG. 9. Correlation of grain size (d50) values, percentage of dry mass, ARM_{30mT}/ARM, and total mercury (TotHg) for each core. The ratio of ARM_{30mT} (after demagnetization) to initial ARM relates the ease or difficulty of sample demagnetization in an alternating field and is a measure of grain size of the magnetic fraction. The abbreviation d50 refers to the median grain size. The ARM_{30mT}/ARM measurements are from the "B" cores (see *Methods*); the magnetic measurements for OA-03B are shorter than the adjacent Oaks Arm cores due to over-penetration of the B core. Percentage of dry mass and TotHg measurements are from Richerson et al. (2008). The 1954 horizon was projected onto OA-03C from the companion core OA-03A, where the dichlorodiphenyldichloroethane (DDD) concentrations were actually measured.

lake at the angle of repose (Suchanek et al. 2003, 2008*b*). Most of the waste rock was bulldozed into place during the main open-pit mining phase from 1927 to 1944 (Chamberlin et al. 1990). The total annual erosion loss from the waste pile was ~50 000 Mg/yr (Richerson et al. 1994) prior to the emplacement of riprap along the base of the pile by the U.S. Environmental Protection Agency (U.S. EPA) in 1992. Erosion of coarse particles likely occurred by sheetwash along the steeply sloping outer surface of the piles as well as by mass wasting of the outer surface induced by wave undercutting along the waterline (Richerson et al. 2000). Surface currents in Clear Lake are driven by dominant winds from the northwest that transform seasonally into a strong, bottom-hugging countercurrent that flows west-northwest back into the other arms of the lake (Lynch and Schladow 1997, Rueda et al. 2008). Maximum current velocities of 11–19 cm/s occur during August in Clear Lake (Rueda et al. 2008), sufficient to move coarse silts and fine sands throughout the Oaks Arm and finer sediment and contaminants farther out into the Upper and Lower Arms. Thus, the initial post-1927 coarsening-upward trend in the Oaks Arm core is consistent with proposed hypotheses relating the coincident environmental changes recorded in numerous chemical and ecological parameters to the advent of open-pit Hg mining (Richerson et al. 1994, 2000, 2008). Indeed, the sheer volume of sediment transported to the lake after 1927 represents an enormous, abrupt pulse of deposition unlike anything ever experienced by the lake prior to this time.

The turnaround in median grain size in OA-03C from coarsening- to fining-upward (at ~70 cm depth; Fig. 9) also correlates relatively closely with an abrupt decrease in TotHg. The turnaround occurs just above the estimated date of 1954 determined from a sharp DDD spike measured in companion core OA-03A (Richerson et al. 2008). We speculate that the shift from coarsening- to fining-upward grain size patterns in this core records the final termination of open-pit mining operations (and associated flux of mechanically introduced coarse sediment) at the mine ca. 1957. Furthermore, sedimentation rates decrease above this 1954 datum, from 18–20 mm/yr below to ~2–4 mm/yr above, lending further support to a connection with the termination of open-pit mining practices at Sulphur Bank.

Upper Arm.—The post-1927 abrupt fining-upward pattern in the Upper Arm core seems contradictory given the proposed mechanism just discussed for the upward coarsening in the Oaks Arm (Figs. 3D and 9). Our model for the textural trend in UA-03 is also associated with anthropogenic influences, but is only peripherally related to Hg mining at Sulphur Bank. Beginning in the 1920s, several changes in land use occurred in the Clear Lake basin, including a road-building boom, the filling of wetlands, mining for aggregate from stream beds, and recreational development near the lake, all involving the use of heavy earthmoving equipment (Goldstein and Tolsdorf 1994, Richerson et al. 1994, Suchanek et al. 2003). The net effect of these human-induced changes in the watershed was to increase erosion rates (especially of soils and surficial sediments) and thus increase the sediment supply and nutrient load into the lake. Three indirect lines of evidence support the interpretation of an abrupt increase in erosion/sedimentation rates beginning in the 1920s, corroborating the 10-fold change in rates calculated by ^{14}C dating (below the 1927 horizon) and ^{210}Pb dating (above the 1927 horizon). (1) The UA-03 and OA-03C cores exhibit sharp increases in percentage of dry mass above the 1927 datum (Fig. 9), a dramatic change from the expected progressive decrease in dry mass predicted from the pre-1927 trend (Richerson et al. 2008). (2) Total organic carbon, total organic content (represented by percentage of loss on ignition), and total nitrogen sharply decrease commencing near the 1927 datum (Richerson et al. 2000, 2008), indicating dilution by an increased flux of inorganic sediment into the lake. (3) The abrupt increase in magnetic concentration and the parallel decrease in the size of magnetic grains after 1927 in UA-03 point toward the inhibition of magnetite dissolution due to rapid burial, as discussed in the *Oaks Arm* section above. Using dates estimated from the Hg and DDD datums (Richerson et al. 2008), sedimentation rates in UA-03 were highest between 1927 and 1954, ~24 mm/yr, whereas post-1954 rates are ~2–4 mm/yr. The abrupt change in rate around the early to mid-1950s suggests that the range of rates from 1927 to 2000 determined from ^{210}Pb dating for all three arms of the lake (5.5–12.2 mm/yr) are long-term averages (Richerson et al. 2008).

The post-1927 fining-upward trend in UA-03 is somewhat counterintuitive in that the traditional pattern in many stratigraphic successions is that increasing discharge or erosion rate in the catchment area produces an increase in grain size in the basin. We suggest that the decrease in grain size post-1927 is due to the preferential erosion of fine-grained soils and shallowly buried sediments by earthmoving equipment, exacerbated by streambed mining of coarse sediment and wetlands destruction (Suchanek et al. 2003). The Franciscan source rocks in the region supply naturally fine-grained material for soils in northern California (Popenoe et al. 1992). Alluvial storage and attendant chemical weathering of particles during residence in soil horizons contributes to their overall diminution by the creation of clays and the production of easily abraded weathering rinds around particles. In the case of the Scotts Creek and Middle Creek drainages, their flow crosses clay loam soils dominated by clays, silts, and very fine sands (Carpenter et al. 1927). Grain size measurements of these soils by Carpenter et al. (1927) yielded typical values of ~2–7% coarse sand, 2–9% medium sand, 5–12% fine sand, 14–20% very fine sand, 25–50% silt, and 21–32% clay. Fig. 4 illustrates the fine-grained sizes of the inorganic particles (including silicate grains) in core UA-03A. The d50 grain sizes in the fine-to-medium silt

range likely reflect their origin from Franciscan-derived soils mantling the watershed around the Upper Arm.

Road-building and associated cut-and-fill activities began in earnest in the 1920s (Richerson et al. 2000). Carpenter et al. (1927:8) state, "there are no paved roads in the area, but all principal highways are graveled." The 1927 reopening of Sulphur Bank Mercury Mine stimulated lakeshore development and the growth of small communities linked by paved roads. Large quantities of fine-grained soils and surficial sediments disturbed by heavy earthmoving equipment likely ended up entering the Upper Arm of the lake and contributed to the fining upward trend evident in UA-03. Not only were finer-grained sediments entering the lake in greater quantities post-1927, but coarser-grained sediments were not being deposited in the lake, as evidenced by the dramatic decrease in the d90 fraction in UA-03 (Fig. 3C). This pattern is likely related to streambed gravel mining, effectively reducing coarse sediment input to the lake. This gravel mining occurred from the 1920s to the 1980s (Suchanek et al. 2003) and resulted in a number of ancillary effects that appear to be recognizable in lake bottom sediments. Mining sites destabilized upstream and downstream channel morphology, impacting riparian vegetation and making streambanks vulnerable to undercutting and erosion (Follansbee and Why 1994). Floodplain farms and streamside terraces became exposed to erosion during flood flows, increasing the flux of fine-grained alluvial soils into the streams and ultimately to the lake (Follansbee and Why 1994). Other land use practices initiated in the 1920s that increased overland flow from catchment slopes and thus the nature of sediment entering the lake include extensive clearing of steep slopes for walnut orchards, steep road cuts along the lake shore, and dirt roads in upland areas (Follansbee and Why 1994, Suchanek et al. 2003, Richerson et al. 2008).

Another factor that contributed to the fining-upward trend in UA-03 in both the inorganic and organic fractions beginning in the late 19th century (Fig. 4) was the destruction of wetlands, especially those at the northwest corner of Clear Lake where Scotts Creek and Middle Creek join before entering the lake through Rodman Slough. Over 809 ha of wetlands were lost, along with their nutrient- and sediment-trapping abilities (Richerson et al. 2000, Suchanek et al. 2003). Flood flows from the Scotts Creek and Middle Creek drainages, along with their entrained fine sediment and nutrients, now directly enter the lake, resulting in the aggradation of the delta at the mouth of Rodman Slough (Follansbee and Why 1994). The flux of flocculated clay and silt particles into the Upper Arm after 1927 likely carried nutrients (e.g., phosphorus) and trace elements (e.g., iron) that acted as catalysts to cyanobacterial growth (Richerson et al. 1994, Kim 2003). Diatom productivity declined in an irregular pattern after 1927, perhaps related to enhanced competition from cyanobacterial blooms driven by the increased sediment supply/nutrient load (Richerson et al. 1994, Suchanek et al. 2003). This is supported by a reduction in the N/P ratio after 1927 (Richerson et al. 2008), a trend that may indicate increased nitrogen fixation by cyanobacteria (Smith 1983). The historically documented algal blooms of the mid- to late 20th century acted to increase the autochthonous biomass that combined with the inorganic sediment supply from the watershed. Both of these components contributed to the 10-fold increase in sedimentation rate and C mass accumulation rate after 1927 (Richerson et al. 2008).

Conclusions

The results of our textural and magnetic investigations of Clear Lake bottom sediments point to a major anthropogenic influence over the past 80 or so years of sediment accumulation. The collective effects of open-pit mining, road building, stream bed mining for aggregate, and wetlands destruction are clearly recorded in the textural and magnetic signatures of the lake sediment. In concert with the concurrent shifts in ecological and chemical parameters recognized by coworkers (Richerson et al. 2008), these data strongly support hypotheses previously suggested for the abrupt environmental shifts wrought by wholesale land use changes in the Clear Lake basin since the 1920s. In sum, the cultural eutrophication (Smith 1998) of Clear Lake began with the advent of large-scale open-pit Hg mining in 1927 and subsequent human-induced landscape modification involving heavy earthmoving equipment. These activities resulted in increased erosion/sedimentation rates and associated nutrient input to the lake, culminating in algal blooms and reduced surface water quality through the rest of the 20th century.

Acknowledgments

We thank Neil Tabor for assistance in the laboratory and Ken Verosub for use of the magnetics laboratory at UC–Davis. Tom Guilderson of Lawrence Livermore National Lab aided in the interpretation of the radiocarbon dates. The comments of two anonymous reviewers improved the paper significantly, as did feedback from U.S. Geological Survey (USGS) reviewers Julie Yee and Karen Phillips. This work was supported by the U.S. EPA-funded (R819658 and R825433) Center for Ecological Health Research at UC–Davis, U.S. EPA Region IX Superfund Program (68-S2-9005), UC–Davis, and the U.S. Geological Survey (Western Ecological Research Center). Although portions of this work have been funded wholly or in part by the U.S. Environmental Protection Agency, it may not necessarily reflect the views of the Agency, and no official endorsement should be inferred. Any use of trade, product, or firm names in this publication is for descriptive purposes only and does not imply endorsement by the U.S. government.

Literature Cited

Bergfeld, D., F. Goff, and C. J. Janik. 2001. Carbon isotope systematics and CO_2 sources in the Geysers-Clear Lake region, northern California, USA. Geothermics 30:303–331.

Bleil, U. 2000. Sedimentary magnetism. Pages 73–83 *in* H. D. Schultz and M. Zabel, editors. Marine geochemistry. Springer-Verlag, Berlin, Germany.

Canfield, D. E., and R. A. Berner. 1987. Dissolution and pyritization of magnetite in anoxic marine sediments. Geochimica et Cosmochimica Acta 51:645–659.

Carpenter, E. J., R. E. Storie, and S. W. Cosby. 1927. Soil survey of the Clear Lake area, California. Number 13. Bureau of Chemistry and Soils, U.S. Department of Agriculture, Washington, D.C., USA.

Chamberlin, C. E., R. Chaney, B. Finney, M. Hood, P. Lehman, M. McKee, and R. Willis. 1990. Abatement and control study: Sulphur Bank Mine and Clear Lake. Environmental Resources Engineering Department, Humboldt State University, Arcata, California, USA.

Channell, J. E. T., and J. S. Stoner. 2002. Plio-Pleistocene magnetic polarity stratigraphies and diagenetic magnetite dissolution at ODP Leg 177 Sites. Marine Micropaleontology 45:269–290.

Cook, A. C., L. J. Hainsworth, M. L. Sorey, W. C. Evans, and J. R. Southan. 2001. Radiocarbon studies of plant leaves and tree rings from Mammoth Mountain, CA: a long-term record of magmatic CO_2 release. Chemical Geology 177:117–131.

Follansbee, B. A., and S. Why. 1994. Wetlands and riparian vegetation. Pages VIII-1–VIII-6 *in* P. J. Richerson, T. H. Suchanek, and S. J. Why, editors. The causes and control of algal blooms in Clear Lake: clean lakes diagnostic/feasibility study for Clear Lake, California. Final Report. Division of Environmental Studies, University of California, Davis, California, USA.

Goldman, C. R., and R. G. Wetzel. 1963. A study of the primary productivity of Clear Lake, Lake County, California. Ecology 44:283–294.

Goldstein, J. J., and T. N. Tolsdorf. 1994. An economic analysis of potential water quality improvement in Clear Lake. Benefits and costs of sediment control, including a geological assessment of potential sediment control levels. Final Report. Division of Environmental Studies, University of California, Davis, California, USA.

Hearn, B. C., R. J. McLaughlin, and J. M. Donnelly-Nolan. 1988. Tectonic framework of the Clear Lake basin, California. Pages 9–20 *in* J. D. Sims, editor. Late Quaternary climate, tectonism, and sedimentation in Clear Lake, northern California Coast Ranges. Special Paper 214. U.S. Geological Survey, Menlo Park, California, USA.

Karlin, R., and S. Levi. 1983. Diagenesis of magnetic minerals in recent hemipelagic sediment. Nature 303:327–330.

Kim, J. G. 2003. Response of sediment chemistry and accumulation rates to recent environmental changes in the Clear Lake watershed, California, USA. Wetlands 23:95–103.

Lynch, M. G., and S. G. Schladow. 1997. Clear Lake current study: mixing and transport dynamics. Special Report Number EDL96-01MGL. Attachment 2 *in* T. H. Suchanek, et al., editors. The role of the Sulphur Bank Mercury Mine site in the dynamics of mercury transport and bioaccumulation within the Clear Lake aquatic ecosystem. U.S. Environmental Protection Agency Region IX Superfund Program, San Francisco, California, USA.

Mack, E. E. 1998. Sulfate reduction and mercury methylation potential in the sediments of Clear Lake (CA). Dissertation. University of California, Davis, California, USA.

Pasquier-Cardin, A., P. Allard, T. Ferreira, C. Hatte, R. Coutinho, M. Fontugne, and M. Jaudon. 1999. Magma-derived CO_2 emissions recorded in ^{14}C and ^{13}C content of plants growing in Furnas caldera, Azores. Journal of Volcanology and Geothermal Research 92:195–207.

Popenoe, J. H., K. A. Bevis, B. R. Gordon, N. K. Sturhan, and D. L. Hauxwell. 1992. Soil-vegetation relationships in Franciscan terrain of northwestern California. Soil Science Society of America Journal 56:1951–1959.

Richerson, P. J., T. H. Suchanek, J. C. Becker, A. C. Heyvaert, D. G. Slotton, J. G. Kim, X. Li, L. M. Meillier, D. C. Nelson, and C. E. Vaughn. 2000. The history of human impacts in the Clear Lake watershed (California) as deduced from lake sediment cores. Pages 119–145 *in* K. M. Scow, G. E. Fogg, D. E. Hinton, and M. L. Johnson, editors. Integrated assessment of ecosystem health. Lewis, Washington, D.C., USA.

Richerson, P. J., T. H. Suchanek, and S. J. Why. 1994. The causes and control of algal blooms in Clear Lake: clean lakes diagnostic/feasibility study for Clear Lake, California. Final Report. Division of Environmental Studies, University of California, Davis, California, USA.

Richerson, P. J., T. H. Suchanek, R. A. Zierenberg, D. A. Osleger, A. C. Heyvaert, D. G. Slotton, C. A. Eagles-Smith, and C. E. Vaughn. 2008. Anthropogenic stressors and changes in the Clear Lake ecosystem as recorded in sediment cores. Ecological Applications 18(Supplement):A257–A283.

Robinson, S. W., D. P. Adams, and J. D. Sims. 1988. Radiocarbon content, sedimentation rates, and a time scale for core CL-73-4 from Clear Lake, California. Pages 151–160 *in* J. D. Sims, editor. Late Quaternary climate, tectonism, and sedimentation in Clear Lake, northern California Coast Ranges. Special Paper 214. U.S. Geological Survey, Menlo Park, California, USA.

Rueda, F. J., S. G. Schladow, and J. F. Clark. 2008. Mechanisms of contaminant transport in a multi-basin lake. Ecological Applications 18(Supplement):A72–A87.

Shipp, W. G., and R. A. Zierenberg. 2008. Pathways of acid mine drainage to Clear Lake: implications for mercury cycling. Ecological Applications 18(Supplement):A29–A54.

Sims, J. D., M. J. Rymer, and J. A. Perkins. 1988. Late Quaternary deposits beneath Clear Lake, California: physical stratigraphy, age, and paleogeographic implications. Pages 21–44 *in* J. D. Sims, editor. Late Quaternary climate, tectonism, and sedimentation in Clear Lake, northern California Coast Ranges. Special Paper 214. U.S. Geological Survey, Menlo Park, California, USA.

Smith, V. H. 1983. Low nitrogen to phosphorous ratios favor dominance by blue-green algae in lake phytoplankton. Science 221:669–671.

Smith, V. H. 1998. Cultural eutrophication of inland, estuarine and coastal waters. Pages 7–49 *in* M. L. Pace and P. M. Groffman, editors. Successes, limitations and frontiers in ecosystem science. Springer, New York, New York, USA.

Stuiver, M., P. J. Reimer, and R. W. Reimer. 2005. CALIB 5.02. Program and documentation. ⟨http://www.calib.qub.ac.uk/crev50/⟩

Suchanek, T. H., P. J. Richerson, L. J. Mullen, L. L. Brister, J. C. Becker, A. Maxson, and D. G. Slotton. 1997. The role of the Sulphur Bank Mercury Mine site (and associated hydrogeological processes) in the dynamics of mercury transport and bioaccumulation within the Clear Lake aquatic ecosystem. U.S. Environmental Protection Agency, Region IX Superfund Program, San Francisco, California, USA.

Suchanek, T. H., P. J. Richerson, R. A. Zierenberg, D. G. Slotton, and L. H. Mullen. 2008*a*. Vertical stability of mercury in historic and prehistoric sediments from Clear Lake, California. Ecological Applications 18(Supplement): A284–A296.

Suchanek, T. H., et al. 2003. Evaluating and managing a multiply stressed ecosystem at Clear Lake, California: a holistic ecosystem approach. Pages 1239–1271 *in* D. J. Rapport, W. L. Lasley, D. E. Rolston, N. O. Nielsen, C. O. Qualset, and A. B. Damania, editors. Managing for healthy ecosystems. Lewis, Boca Raton, Florida, USA.

Suchanek, T. H., et al. 2008*b*. The legacy of mercury cycling from mining sources in an aquatic ecosystem: from ore to organism. Ecological Applications 18(Supplement):A12–A28.

Thompson, R., and F. Oldfield. 1986. Environmental magnetism. Allen and Unwin, Boston, Massachusetts, USA.